## Analysis of a microelectromechanical system testing stage for tensile loading of nanostructures

Shaoning Lu, Zaoyang Guo, Weiqiang Ding, and Rodney S. Ruoff<sup>a)</sup>
Department of Mechanical Engineering, Northwestern University, 2145 Sheridan Road, Evanston, Illinois 60208-3111

(Received 5 August 2005; accepted 26 March 2006; published online 5 May 2006)

A new analytical model is developed for interpreting tensile loading data on "templated carbon nanotubes" (T-CNTs, amorphous carbon nanotubes made by pyrolysis with the channels of nanopores in anodized alumina nanopore arrays) obtained with a microelectromechanical-system (MEMS)-based mechanical testing stage. It is found that the force output from the actuation unit of the testing stage depends on the stiffness of the force sensing beam and the nanostructure being loaded, as well as the power input. A superposition method is used to treat the mechanics of the device structure in the linear elasticity response regime. To our knowledge this is a new approach for solving the mechanical response of MEMS structures with variable force output and of the configuration described herein. An in situ mechanical testing of individual T-CNTs was undertaken in a scanning electron microscope (LEO1525) using a new device fabricated with integrated electrodes for controlled deposition of T-CNTs by electric-field guided assembly in a liquid. The T-CNT was subsequently tensile loaded to the point of fracture. The calculated modulus of the T-CNT using the new model based on the experimentally measured displacement of the moving platform with and without the T-CNT attached falls within the range expected for amorphous carbon. The new model corrects the treatment in a previously presented model [S. Lu et al., Rev. Sci. Instrum. 75, 2154 (2004)]. © 2006 American Institute of Physics.

[DOI: 10.1063/1.2198789]

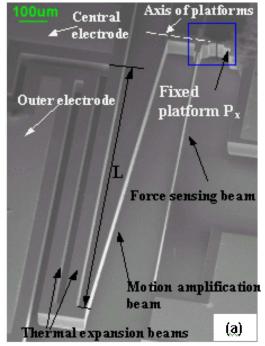
A microelectromechanical-system (MEMS)-based testing stage for measuring the mechanical properties of nanostructures was previously presented. Nanometer scale displacement resolution was obtained when testing the device in a scanning electron microscope (SEM) but without nanostructures attached. The device consists of a thermal actuator coupled to a motion amplification structure and an indirect force sensing beam. A method was developed for electricfield guided assembly of nanowires such as templated carbon nanotubes (T-CNTs),<sup>2</sup> and then put to use with this tensile loading device by fabrication of optimized platforms, electrodes, and circuits. It has become apparent that a new model for obtaining Young's modulus of nanowires or nanotubes loaded with this testing stage was needed to correctly treat the device and nanostructure mechanics during actuation. This new model may be of use for other MEMS devices having nonlinear force output. Thus, the primary focus of this article is the presentation of this new model. We note for the reader that T-CNTs are not particularly uniform with respect to cross section along their length, but they were used here because of our prior experience in readily identifying their deposition through electric-field guided assembly with optical microscopy, which led to the realization that a new treatment of the device function (its mechanics) was called

Figure 1(a) shows the new device having the integrated electrodes. The thickness of the structures is  $100 \mu m$ , and

the distance between the silicon platforms (attached to the moving and fixed platforms, respectively) is 6  $\mu$ m, chosen from separate optimization of the electric-field guided assembly process of deposition. Au electrodes were patterned on top of the silicon platforms for aligning and attaching T-CNTs by dielectrophoretic deposition. Details regarding the design, fabrication, and process of dielectrophoretic deposition are described in our previous work.<sup>2,3</sup> A T-CNT deposited across the two platforms of the testing stage is shown in Fig. 1(b). The amorphous T-CNTs were made by pyrolyzing ethylene in alumina nanopore membranes.<sup>4</sup> After deposition, the T-CNT was clamped at each platform by making a carbonaceous deposit with the electron beam induced decomposition (EBID) method. 3,5,6 By applying current through the thermal expansion beams, the device is actuated and the platform  $P_m$  (the "moving platform") is pulled toward the left in Fig. 1. A tensile load is thereby applied to the T-CNT attached between platform  $P_m$  and the opposing fixed platform  $(P_f)$ . The displacement of platform  $P_m$  will differ depending on whether a T-CNT is attached across the two platforms. By knowing the device mechanics and by measuring displacement with and without the nanostructure (here, T-CNT) the stiffness and modulus of the T-CNT could be obtained, based on the following model.

We first define the device as consisting of two different functional units. The *actuation unit* is composed of the thermal expansion beams and the motion amplification beam [Figs. 1(a) and 2]. The indirect force sensing beam and the attached specimen (T-CNT in this case) are the *measurement unit*. The force output from the actuation unit is the load

a) Author to whom correspondence should be addressed; electronic mail: r-ruoff@northwestern.edu



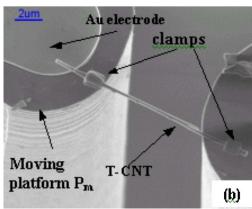


FIG. 1. (Color online) (a) SEM image of an improved tensile loading device for measuring the mechanics of nanostructures. The device is symmetric so half of it is shown here. The length of the thermal expansion beam is 1022  $\mu$ m, the width is 48  $\mu$ m, and the thickness is 100  $\mu$ m. The total resistance of the thermal expansion beams (half of the symmetrical device) is 85  $\Omega$ . The device is operated by grounding the central electrical pad and the outer electrodes are at the same potential. (b) A T-CNT assembled across the platforms of the testing stage in (a). The average outer diameter (o.d.) of the T-CNT is 330 nm, the average inner diameter (i.d.) is 163 nm, and the length between the clamps prior to loading is 10  $\mu$ m. The average cross sectional area is  $6.5 \times 10^{-14}$  m<sup>2</sup> (Ref. 7).

applied to the measurement unit. We note that the (secant) stiffness of a structure is defined as the force divided by the displacement (along a particular direction at a particular point) caused by the force (only). The force used to define the stiffness of the actuation unit  $(K_d)$  is its output force applied to the measurement unit, while the corresponding displacement is the displacement of this unit at point A [Fig. 2(a)] caused by this force only (along the axis of the opposing platforms). The displacement x that is experimentally measured at the moving platform  $P_m$  is not caused by the output force only, as discussed in detail below. The displacement x, used for defining the stiffness of the measurement unit, is the horizontal displacement at the midpoint of the force sensing beam (on the moving platform), which is

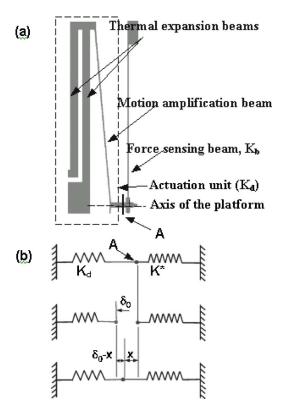


FIG. 2. (Color online) (a) Schematics of the device and (b) an equivalent spring system.  $K_d$  is the stiffness of the actuation unit, and  $K^* = K_h$  (without T-CNT attached) or  $K^* = K_b + K_s$  (with T-CNT attached). In illustration (a), the nanostructure is not loaded.

equivalent to the actual displacement x of point A that we measured. Obviously, the corresponding force for the measurement unit is equal to the value of the output force of the actuation unit. Hence, the stiffness of the measurement unit is  $K^* = K_b$  (without the attached specimen) or  $K^* = K_b + K_s$ (with specimen attached, i.e., the clamped, clamped boundary condition), where  $K_b$  is the stiffness of the indirect force sensing beam, and  $K_s$  is the stiffness of the specimen (T-CNT).

The force output from the actuation unit depends on the stiffness of the measurement unit as well as the power input. Thus, at a particular power input, the force output can be written as  $F = f(K^*)$ . If the stiffness of the measurement unit changes as a consequence of the loading from different nanostructures, then the force output from the actuation unit (at point A) will change as well, even if the actuation unit has the same power input from the power supply.

A previous model assumed that, for a certain power input, the force output at point A was constant. This assumption was found to be not valid for the mechanical structure of this testing stage, which can be proved by considering an asymptotic case. If this assumption were true at a particular power input, it would mean that the displacement of the measurement unit is inversely proportional to the stiffness of the force sensing beam  $K_b$ . If this were true, when the stiffness  $K_b$  approaches zero, the displacement would be infinitely large. However, the displacement (x) would not be infinitely large for a given power input, because it is limited by the structure of the actuation unit. Hence the reported method of calculating the stiffness of a nanostructure loaded with this device is not correct and we provide the correct model here.

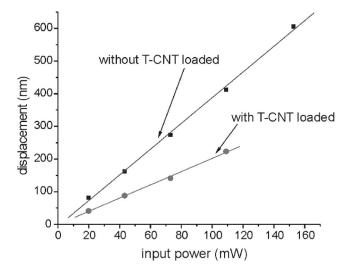


FIG. 3. Displacement of the moving platform when a T-CNT is, and is not, loaded.

By the definition of the measurement unit stiffness  $K^*$ , the displacement x satisfies  $K^*x=F$ , where x cannot be obtained when  $K^*=0$ . The value of x can only be obtained by making an imaginary cut at point A that separates the actuation unit and the measurement unit, with the temperature distribution and thermal boundary condition not changed, as before this imaginary cut. For this imaginary situation, F =0. The actuation unit will move (to the left) toward the central pad a certain distance after this imaginary cut. We call this imaginary situation the free status and denote the displacement of the actuation unit at this free status as  $\delta_0$ . It should be noted that even though the output force of the actuation unit is zero, there does exist thermal stress due to the power input. Obviously, the value  $\delta_0$  depends on the power input, and the larger the power input, the larger is  $\delta_0$ . Because the nanostructures we tested are very slim, we assume that the effect of the nanostructure on the temperature distribution and thermal boundary conditions of the silicon structure can be ignored. As we will show below, the deformation of the silicon structures is very small and can therefore be treated as within the linear elasticity regime. Therefore, the effect of the device deformation on the temperature distribution is negligible. Hence,  $\delta_0$  only depends on the amount of power input.

During our testing, the silicon structure is elastic before the specimen (T-CNT) is broken as the whole structure returns to the original configuration when the input power is reduced to zero. The system is in the linear elastic regime because (1) the strains in the silicon structure estimated from the measured displacements are within the linear elastic regime of the material (<0.001% in the force sensing beam), (2) numerical simulation shows that the whole structure is within the linear elastic regime, and (3) the experimental results in Fig. 3 also confirm the linear relation between the load (power input) and the response (the displacement). Hence, the well-known principle of superposition in the linear elastic regime can be applied.

Thus in the real situation, the displacement of the actuation unit can be divided into two parts: one is caused by the thermal stress in the free status and the other is caused by the force applied by the measurement unit, which is equal to the output force F. As explained above, the first part of the displacement is  $\delta_0$  of the free status. The second part of the displacement can be computed based on the original (undeformed) structure, since the effect of the small displacement  $\delta_0$  can be ignored in linear elasticity theory. Because the change of silicon modulus is less than 5% between 300 and 850 K, 10,11 it is acceptable to ignore the difference in the moduli of the silicon structure caused by slight changes in temperature. Thus, the secant stiffness of the actuation unit  $K_d$  can be considered as a constant because of the linear elasticity. Similarly the secant stiffness of the indirect force sensing beam  $K_b$  is also a constant. Thus, the system can be simplified as shown in the spring diagram [Fig. 2(b)], in which the actuation unit is represented as a spring (loading device spring) with a constant stiffness  $K_d$ , while the measurement unit is simplified as a "measurement" spring with stiffness  $K^*$ .

As stated above, if the two springs are hypothetically separated, the distance between the two resulting relaxed springs is  $\delta_0$ , which depends on the magnitude of the input power. The total displacement x of the actuation unit is then

$$x = \delta_0 - F/K_d. \tag{1}$$

This displacement is equal to the displacement of the measurement unit, so

$$x = F/K^*. (2)$$

When the device is actuated and no nanostructures are loaded, as in Fig. 2(b), the actuation unit is loaded with a force from the force sensing beam only. The force output from the actuation device  $F_1$  can be derived from (1) and (2),

$$F_1 = K_d(\delta_0 - x_1) = K_b x_1, \tag{3}$$

where  $x_1$  is the deformation of the force sensing beam. When a nanostructure (T-CNT) is attached, the displacement of the measurement unit is  $x_2$ , and by applying Eqs. (1) and (2), we have

$$F_2 = K_d(\delta_0 - x_2) = (K_b + K_s)x_2, \tag{4}$$

and with Eq. (3), we obtain

$$K_s = (K_d + K_h)(x_1 - x_2)/x_2,$$
 (5)

which indicates

$$\frac{x_1 - x_2}{x_2} = \frac{K_s}{K_d + K_b} = \text{const.}$$
 (6)

With this solution, we tested a T-CNT in Fig. 1 with monotonically increasing power inside the SEM. The instrumentation and testing procedure are described by Lu et al.<sup>3</sup> The current was adjusted in 10 mA increments in constant current mode while the voltage was recorded from the same power supply (HP6613 dc; Hewlett Packard). The elongation of this T-CNT was repeatable below 109 mW during three such tensile loading experiments. The T-CNT was broken when the power reached 153 mW during the third experiment. No slippage was observed between the T-CNT, the clamps, and the platform surfaces. The displacement of the moving platform was obtained by measuring the elongation of the T-CNT, since the other end of the T-CNT was clamped on the fixed platform. The T-CNT elongation was measured between the inner edges of the clamps at each input power, from the SEM images. After fracturing the T-CNT, the displacement of the moving platform without any attached T-CNT was measured at the same intervals of power input, by following the sharp features on the sidewall of the platform  $P_m$  with the method reported previously. The experimentally measured displacement of the moving platform  $P_m$  with (x') and without (x) the T-CNT attached is shown in Fig. 3.

The stiffness of the actuation device  $K_d$  and the force sensing beam  $K_b$  can be calculated by using the finite element analysis software ABAQUS, with the actual dimensions of the device as measured in the SEM. From the experimental results displayed in Fig. 3, the average  $(x_1-x_2)/x_2$  is 0.75. The computed stiffness of the actuation device is  $K_d = 5.6$  $\times 10^2$  N/m, and the stiffness of the force sensing beam is  $K_b$ =2.8 N/m; the modulus E=169 GPa [(110) direction<sup>9</sup>] is used for silicon because the device is fabricated such that the long beams (thermal expansion beam, indirect force sensing beams) are along the (110) direction. Substituting into Eq. (6), we obtain  $K_s = 4.2 \times 10^2$  N/m. Ultimately, the modulus of the T-CNT is determined to be  $E_s = K_s L_s / A_s = 66$  GPa, where dimensions of the T-CNT are derived from SEM images such as the one shown in Fig. 1. This is a typical value for such T-CNTs, as discussed next.

The T-CNTs were also tested independently with the use of atomic force microscopy (AFM) cantilevers attached to a nanomanipulator in the SEM. The testing procedure is the same as previously used for multiwall carbon nanotubes and amorphous carbon nanocoils. 6,12,13 A T-CNT was attached between two opposing AFM tips, with each end of the T-CNT clamped onto the AFM cantilever tips by the EBID method.<sup>5</sup> One of the cantilevers is relatively stiff (k = 14.0 N/m) and the other one is relatively soft (k=0.3 N/m, both on chip NSC12: MikroMasch Inc.). A tensile load is applied to the T-CNT when the soft cantilever is moved away from the stiff cantilever through nanomanipulation. This compliant cantilever is used as the force sensing element, and the force applied on the T-CNT can be obtained from the amount of bending by using the beam theory. The modulus values obtained for the T-CNTs were 30, 45, and 23 GPa for three different T-CNTs. As mentioned, these T-CNTs have an amorphous structure, 4 and we note that the T-CNTs may possibly contain hydrogen, that is, might be comprised of hydrogenated amorphous carbon.

In summary, a new model of a MEMS-based nanomechanical testing stage has been developed to interpret the experimental data and extract the modulus of a nanostructure, here a T-CNT, being tested with the stage. It is found that the force output from the actuation unit depends on the stiffness of the force sensing beam and the nanostructure specimen, as well as the power input. A superposition method was applied for analyzing the device response in the linear elasticity regime. To our knowledge, this is a new treatment of such a loading configuration and experiment. The results provided by a previous model<sup>1</sup> are thus corrected.

The authors gratefully acknowledge D. R. Cantrell for comments. The authors appreciate the support from the Naval Research Laboratory (Grant No. N00173-04-2-C003), the Office of Naval Research (Grant No. N000140210870), and the NSF (CMS-0304506; NIRT: Synthesis, Characterization and Modeling of Aligned Nanotube Arrays for Nanoscale Devices, Ken Chong, program manager). The fabrication work was performed in part at the Cornell Nanoscale Science and Technology Facility (a member of the National Nanofabrication Users Network), which is supported by the National Science Foundation under Grant No. ECS-9731293, its users, Cornell University, and industry affiliates.

<sup>&</sup>lt;sup>1</sup>S. Lu, D. D. Dikin, S. Zhang, F. T. Fisher, J. Lee, and R. S. Ruoff, Rev. Sci. Instrum. **75**, 2154 (2004).

<sup>&</sup>lt;sup>2</sup>S. Lu, J. Chung, and R. S. Ruoff, Nanotechnology **16**, 1765 (2005).

S. Lu, Z. Guo, W. Ding, D. Dikin, J. Lee, and R. S. Ruoff (unpublished).
 T. T. Xu, F. T. Fisher, L. C. Brinson, and R. S. Ruoff, Nano Lett. 3, 1135 (2003).

<sup>&</sup>lt;sup>5</sup> W. Ding, D. A. Dikin, X. Chen, R. D. Piner, X. Wang, X. Li, R. S. Ruoff, and E. Zussman, J. Appl. Phys. **98**, 014905 (2005).

<sup>&</sup>lt;sup>6</sup> M. F. Yu, O. Lourie, M. J. Dyer, K. Moloni, T. F. Kelly, and R. S. Ruoff, Science 287, 637 (2000).

<sup>&</sup>lt;sup>7</sup>The outer diameter is an average of five measured values obtained from SEM images: one near the inner edge of each clamp, one at the region having the smallest apparent value from the images, and one at each of the fracture surfaces. The small branch was not considered. The inner diameter is about half of the outer diameter from the cross section of each fracture surface.

<sup>&</sup>lt;sup>8</sup> Experiments of physically separating the actuation unit and the measurement unit were conducted in SEM under vacuum. It was observed that the displacement at the center of the amplification beam reversed its direction from moving away from the measurement unit to moving toward it, thereby reducing the distance between the two platforms. This was caused by the change of the thermal boundary condition. By detaching the force sensing beam from the actuation unit, heat in the motion amplification beams could not be conducted away to the large Si pad where the force sensing beams were attached. This resulted in an elevated temperature and thermal expansion in the amplification beams. The expansion of the motion amplification beams exceeded the thermal expansion of the heater beams. Therefore, the motion reversed direction. This was also observed by finite element analysis modeling using FEMLAB.

<sup>&</sup>lt;sup>9</sup> J. J. Wortman and R. A. Evans, J. Appl. Phys. **36**, 153 (1965).

<sup>&</sup>lt;sup>10</sup>H. J. McSkimin, J. Appl. Phys. **24**, 988 (1954).

<sup>&</sup>lt;sup>11</sup> S. P. Nikanorov, Y. A. Burenkov, and A. V. Stepanov, Sov. Phys. Solid State 13, 2516 (1971).

<sup>&</sup>lt;sup>12</sup> X. Chen, S. Zhang, D. A. Dikin, W. Ding, and R. S. Ruoff, Nano Lett. 3, 1299 (2003).

<sup>&</sup>lt;sup>13</sup> M. F. Yu, B. S. Files, S. Arepalli, and R. S. Ruoff, Phys. Rev. Lett. **84**, 5552 (2000).